Automatic treatment plan re-optimization for adaptive radiotherapy guided with the initial plan DVHs

2013 Phys. Med. Biol. 58 8725

(http://iopscience.iop.org/0031-9155/58/24/8725)

IOP PUBLISHING PHYSICS IN MEDICINE AND BIOLOGY

Phys. Med. Biol. **58** (2013) 8725–8738 doi:10.1088/0031-9155/58/24/8725

Automatic treatment plan re-optimization for adaptive radiotherapy guided with the initial plan DVHs*

Nan Li[1,2], Masoud Zarepisheh[1], Andres Uribe-Sanchez[1], Kevin Moore[1], Zhen Tian[1], Xin Zhen[1,2], Yan Jiang Graves[1], Quentin Gautier[1], Loren Mell[1], Linghong Zhou[2], Xun Jia[1] and Steve Jiang[1]

[1] Department of Radiation Medicine and Applied Sciences, Center for Advanced Radiotherapy Technologies and University of California San Diego, La Jolla, CA 92037-0843, USA
[2] Department of Biomedical Engineering, Southern Medical University, Guangzhou, Guangdong, 510515, People's Republic of China

E-mail: Steve.Jiang@UTSouthwestern.edu, xunjia@ucsd.edu and smart@smu.edu.cn

Received 15 May 2013, in final form 28 October 2013
Published 4 December 2013
Online at stacks.iop.org/PMB/58/8725

Abstract

Adaptive radiation therapy (ART) can reduce normal tissue toxicity and/or improve tumor control through treatment adaptations based on the current patient anatomy. Developing an efficient and effective re-planning algorithm is an important step toward the clinical realization of ART. For the re-planning process, manual trial-and-error approach to fine-tune planning parameters is time-consuming and is usually considered unpractical, especially for online ART. It is desirable to automate this step to yield a plan of acceptable quality with minimal interventions. In ART, prior information in the original plan is available, such as dose–volume histogram (DVH), which can be employed to facilitate the automatic re-planning process. The goal of this work is to develop an automatic re-planning algorithm to generate a plan with similar, or possibly better, DVH curves compared with the clinically delivered original plan. Specifically, our algorithm iterates the following two loops. An inner loop is the traditional fluence map optimization, in which we optimize a quadratic objective function penalizing the deviation of the dose received by each voxel from its prescribed or threshold dose with a set of fixed voxel weighting factors. In outer loop, the voxel weighting factors in the objective function are adjusted according to the deviation of the current DVH curves from those in the original plan. The process is repeated until the DVH curves are acceptable or maximum iteration step is reached. The whole algorithm is implemented on GPU for high efficiency. The feasibility of our algorithm has been demonstrated with three head-and-neck cancer IMRT cases, each having an initial planning CT scan and another treatment CT scan acquired in the middle of treatment course. Compared with the DVH curves in the original plan, the DVH curves in the

* This work was originally presented at the 54th AAPM annual meeting in Charlotte, NC, July 29–August 2, 2012.

resulting plan using our algorithm with 30 iterations are better for almost all structures. The re-optimization process takes about 30 s using our in-house optimization engine.

(Some figures may appear in colour only in the online journal)

1. Introduction

Adaptive radiotherapy (ART) has the potential of greatly reducing normal tissue toxicity and/or improving tumor control through treatment adaptations based on the up-to-date patient anatomy (Yan *et al* 1997). However, there are still a number of technical limitations preventing ART from clinical implementation (Schwartz 2012). One of the major technical challenges is to develop an effective re-planning method that can generate a new plan recapitulating planning goals in the original IMRT plan in a clinically acceptable time slot and with minimal user intervention.

To achieve these goals, several groups have proposed relatively simple schemes to modify the original plan to account for inter-fraction geometry changes. For example, Court *et al* (2005, 2006) investigated the feasibility of modifying multi-leaf collimator (MLC) leaf positions directly based on the geometrical relationship between the anatomy deformation and the MLC leaves. Mohan *et al* (2005) deformed the intensity patterns according to deformations of anatomy seen in the beam's-eye-view, and then used a leaf sequencing process to generate deliverable MLC segments. Feng *et al* (2006) proposed a direct aperture deformation technique, which first collapsed 3D geometry deformation vector field into a planar 2D vector array, and then used this array to modify the aperture directly. Mestrovic *et al* (2007) studied the feasibility of using direct aperture optimization by using the original plan as the starting point while constraining the search space. Erica *et al* (Ludlum *et al* 2007) developed a simple leaf-tracking algorithm to alter the MLC portal shape directly using the movement information of prostate. Ahunbay *et al* (2008, 2009) also proposed a more sophisticated two-step algorithm, which firstly modify the segments shape based on the geometry changes, and then re-optimize the segment weight for the entire plan. Nonetheless, even though these plan modification methods are efficient in time, to some extent their heuristic nature hinders the optimality of the resulting plans. It is desirable to generate a fully optimized IMRT plan as opposed to heuristically modifying the original one. In this category, Wu *et al* (2008) proposed to deform the dose distribution in the original plan to the current geometry and use it as a target distribution in the optimization. However, this method may be too rigid, in that the deformed dose distribution may not be feasible for the new geometry, especially when the deformation is significant. Fredriksson (2012) also proposed a method to improve plans by using the dose distribution of a previous plan as constraint, which enforce the dose to each voxel or the dose–volume histogram (DVH) of each ROI to be at least as good as in the reference plan, and optimize the sum of the equivalent uniform doses of the OARs. However, their work is to improve the plan quality for the same geometry by optimization under reference dose constraints, which is not working on different geometries for replanning purpose.

In this paper, we propose a method that utilizes DVH in the original plan, which is generated by experienced dosimetrists using a commercial treatment planning system (Eclipse, Varian Medical System, Palo Alto, CA, USA), as guidance for automatic plan re-optimization for ART. The advantages of this approach are twofold. First of all, DVH curves are useful tools for plan evaluation that have direct clinical significance. Since the DVH curves from the original plan imply information of approved dose-volume constraints and represent clinician-approved trade-offs among different structures for this particular patient, we can use them

as the desired DVHs to guide the re-optimization for the patient's new geometry to ensure the clinical acceptability of the new plan. Here, we assume that the original DVHs contain the clinician-approved organ trade-off information and clinically desirable for the patients' new geometry. Second, using DVH information as guidance will give more flexibility for optimization than using dose distribution. It is more likely to reproduce a given DVH than to reproduce a given dose distribution, since the DVH is insensitive to the permutation of voxel doses within each organ.

We achieve the automatic re-planning process by iteratively adjusting voxel-weighting factors in our objective function under the guidance of DVHs. Conventionally, organ-based models have been used, where a single weighting factor is assigned to each organ in the objective function. This essentially treats all voxels within an organ equally, losing a lot of freedom to finely tune the DVH curves. In contrast, voxel-based models tune parameters for each voxel independently. This approach has shown success in many applications (Cotrutz and Xing 2002, 2003, Wu *et al* 2003, Yang and Xing 2004, Shou *et al* 2005, Breedveld *et al* 2007, Lougovski *et al* 2009, 2010). We recently (Zarepisheh *et al* 2012) have also demonstrated mathematically that a voxel-based model explores a much larger Pareto surface than an organ-based model, likely leading to a plan with better trade-off. We also proved that, while the objective function selection is a big concern for the organ-based model, it is no longer an issue for the voxel-based model and the entire large Pareto surface could be explored by using a simple quadratic objective function. It is for these advantages that we employ a voxel-based model with a quadratic objective function in this work and develop an automatic parameter tuning scheme, so that the parameters are adjusted based on the deviation of the original plan's DVHs to the current DVHs.

2. Methods and materials

2.1. Overall re-optimization scheme

We aim at developing an efficient re-optimization algorithm to generate a plan whose DVH is similar or possibly even better than the DVH of the original plan. Our re-optimization algorithm iterates the following two loops. An inner loop is the conventional fluence map optimization, in which we optimize a quadratic objective function penalizing the deviation of the dose received by each voxel from its reference dose with a set of fixed weighting factors. In outer loop, voxel weighting factors in the objective function are adjusted according to the deviation of the DVH curves in the current plan from those in the original plan. The process is repeated until the new plan is close enough to the original plan in terms of the DVH curves, or the maximum iteration step is reached. And the entire process is implemented on GPU for a high efficiency.

2.2. Voxel-based optimization model

Let us denote the set of structures by $S = C \cup T$, where T is the set of targets and C is the set of critical structures, and use v_s to represent the set of voxels in a structure $s \in S$. In our fluence map optimization approach, the number of beamlets is denoted by N and the intensity of beamlets is x_i, $i = 1, 2, \ldots, N$. Then the total dose d_j to a voxel j can be calculated as: $d_j = \sum_i D_{ij} \cdot x_i$, where D_{ij}, the so-called dose deposition coefficient, represents the dose received by the voxel $j \in V$ from the beamlet i of unit intensity. In this study, D_{ij} is computed using our in-house GPU-based dose calculation engine (Gu *et al* 2009, 2011). The following popular two-sided quadratic objective function is employed for this fluence map optimization problem:

$$F_s(d) = \sum_{s \in T} \alpha_s^- \sum_{j \in v_s} (w_j^- \cdot (\max\{0, P_j - d_j\})^2) + \sum_{s \in S} \alpha_s^+ \sum_{j \in v_s} (w_j^+ \cdot (\max\{0, d_j - P_j\})^2) \quad (1)$$

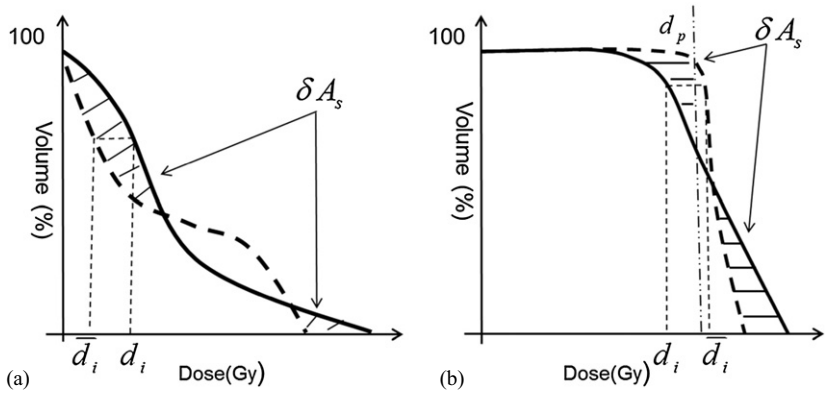

Figure 1. An illustration of DVH comparison for weighting factor adjustment for (a) OAR and (b) PTV. The dashed line is the original DVH and the solid line is the current DVH. The shaded area δA_s represents the area in which the current DVH is worse than the original one for structure s. d_p is the prescription dose. d_i is the current dose value for voxel i and $\bar{d}_i$ is the targeted dose value for this voxel at the next iteration.

where α_s^- and α_s^+ are under-dose and over-dose organ weighting factors, while w_j^- and w_j^+ are those for voxels. P_j denotes the prescription dose for target or threshold dose for critical structures. Given a set of organ and voxel weighting factors, we can find the optimal solution using a gradient projection method (Men *et al* 2009).

2.3. Automatic weighting factor adjustment

Our algorithm starts at solving the fluence map optimization problem with unity weighting factor for each voxel. After that, we adjust the organ and voxel weighting factors by comparing the DVHs of the current solution and the original plan. The weight adjustment is conducted at two stages. At the first several outer iterations, we adjust the organ weighting factors, proportional to the DVH deviation between the current plan and the original one. We call it *the coarse-adjusting stage.* Given that all the voxel weights are the same for each organ at this stage, we are just exploring some parts of the Pareto surface. For the rest of the outer iteration steps, in order to explore the missing parts of the Pareto Surface, each voxel weight is adjusted individually, proportional to the deviation of the current dose to its desirable dose, which will likely improve the plan for better trade-offs. This stage is called *the fine-tuning stage*. Figure 1 illustrates how the DVHs curves are compared to tune the weighting factors. The dashed line is the original DVH and the solid line is the current DVH. The shaded area δA_s represents the area in which the current DVH is worse than the original one for structure s. d_p is the PTV prescription dose. d_i is the current dose value for voxel i. We assign a targeted dose value, $\bar{d}_i$, to this voxel and try to achieve it through the next inner-loop iteration. The value of $\bar{d}_i$ is determined by picking a point on the original DVH that corresponds to the same volume level as d_i on the current DVH, as shown in figure 1. By doing so, the current DVH will be pushed toward the original DVH.

2.3.1. Coarse-adjusting stage. The coarse-adjusting stage is to adjust the organ weighting factors based on δA_s, as shown in figure 1. The exact relationship between the organ weighting factors and the resulting DVH curves is not straightforward. But intuitively, it makes sense to increase the weighting factors for the organs whose DVH curves are far worse than the original ones. This motivates the following weighting factor adjustment:

$$\alpha_s^{k+1} = \alpha_s^k \cdot \left(1 + \frac{\delta A_s}{\sum_{s\varepsilon S} \delta A_s}\right). \tag{2}$$

where δA_s represents how much the current DVH is worse than the original one, and can be defined as:

$$\delta A_s = \int_0^{\max(t)} \delta V_s(t)\, \mathrm{d}t. \tag{3}$$

For OAR, $\delta \mathrm{V}_s(t)$ is defined as:

$$\delta \mathrm{V}_s(t) = \begin{cases} V^{\mathrm{cur}}(t) - V^{\mathrm{org}}(t), & V^{\mathrm{cur}}(t) > V^{\mathrm{org}}(t) \\ 0, & \text{otherwise} \end{cases}, \tag{4}$$

where $V^{\mathrm{cur}}(t)$ and $V^{\mathrm{org}}(t)$ are the volumes of the current and original DVHs at dose level t, respectively. While for PTV, we consider under-dose and over-dose region separately:

$$\delta \mathrm{V}(t) = \begin{cases} V^{\mathrm{org}}(t) - V^{\mathrm{cur}}(t), & (t < d_p) \cap (V^{\mathrm{org}}(t) > V^{\mathrm{cur}}(t)) \\ V^{\mathrm{cur}}(t) - V^{\mathrm{org}}(t), & (t > d_p) \cap (V^{\mathrm{org}}(t) < V^{\mathrm{cur}}(t)) \\ 0, & \text{otherwise} \end{cases}. \tag{5}$$

2.3.2. Fine-tuning stage. The coarse-tuning stage makes the DVH close to the original one. For further improvement, we start to fine-tune the voxel weighting factors. As the DVH is cumulative and insensitive to the locations of the voxel dose values, there are many ways to change the voxel dose values to get a desirable DVH. In our algorithm, to get the desirable DVH, we try to replicate the high (low) dose part of the desirable DVH in those voxels that already receive the high (low) dose values. So, for each voxel, we target a dose value on the desirable DVH that is close to that voxel dose value in the current solution. Then, we increase the voxel weight proportional to the deviation of the current dose to its desirable dose. For a specific voxel j, let d_j^k denote the dose in the voxel j at iteration k, $\mathrm{V}(d_j^k)$ denotes the corresponding volume on the DVH curve for the structure that contains this voxel, and $\bar{d}_j^k$ denotes the dose value corresponding to the value $V(d_j^k)$ on the original DVH curve. Then the weighting factor of this voxel is updated by $w_j^{k+1} = w_j^k \cdot (d_j^k/\bar{d}_j^k)^\mu$ for the over-dose part of PTV and organs at risk, and by $w_j^{k+1} = w_j^k \cdot (\bar{d}_j^k/d_j^k)^\mu$ for the under-dose part of PTV. To avoid having zero values in denominator for the organs at risk, we ignore the very low-dose part of the DVH that has the dose values less than a predetermined threshold value since it is not clinically important. In this work, we set this threshold as 10 cGy. This adjustment is conducted only for the voxels with dose values falling with δA_s, i.e., the regions where the current DVH curve is worse than the original one. The parameter $\mu > 0$ is defined by the user and can affect the convergence behavior of the algorithm. However, based on our experiments, the parameter μ is not case dependent. We can fix it for all the cases, which will be discussed later in the 'Results' section. The rationale for this adjustment is as following. There are apparently a large number of possible dose distributions corresponding to the original DVH curve. However, if we change dose at each voxel j from d_j^k into $\bar{d}_j^k$ following the above mentioned procedure, the resulting dose distribution will have the same, or better DVH curves, as shown in the appendix. Hence, we view $\bar{d}_j^k$ as the targeted dose distribution inferred from the original DVHs and adjust weighting factors to approach it.

2.3.3. Normalization. In order to avoid the numerical errors caused by the presence of very big or very small weighting factors in this automatic weighting factor adjustment procedure, we keep them within a specific range through normalization at each iteration. As such, we normalize weighting factors as follows:

$$w_j^{k+1} = w_j^{k+1} \times \frac{\sum_{j\in V} w_j^k}{\sum_{j\in V} w_j^{k+1}}. \tag{6}$$

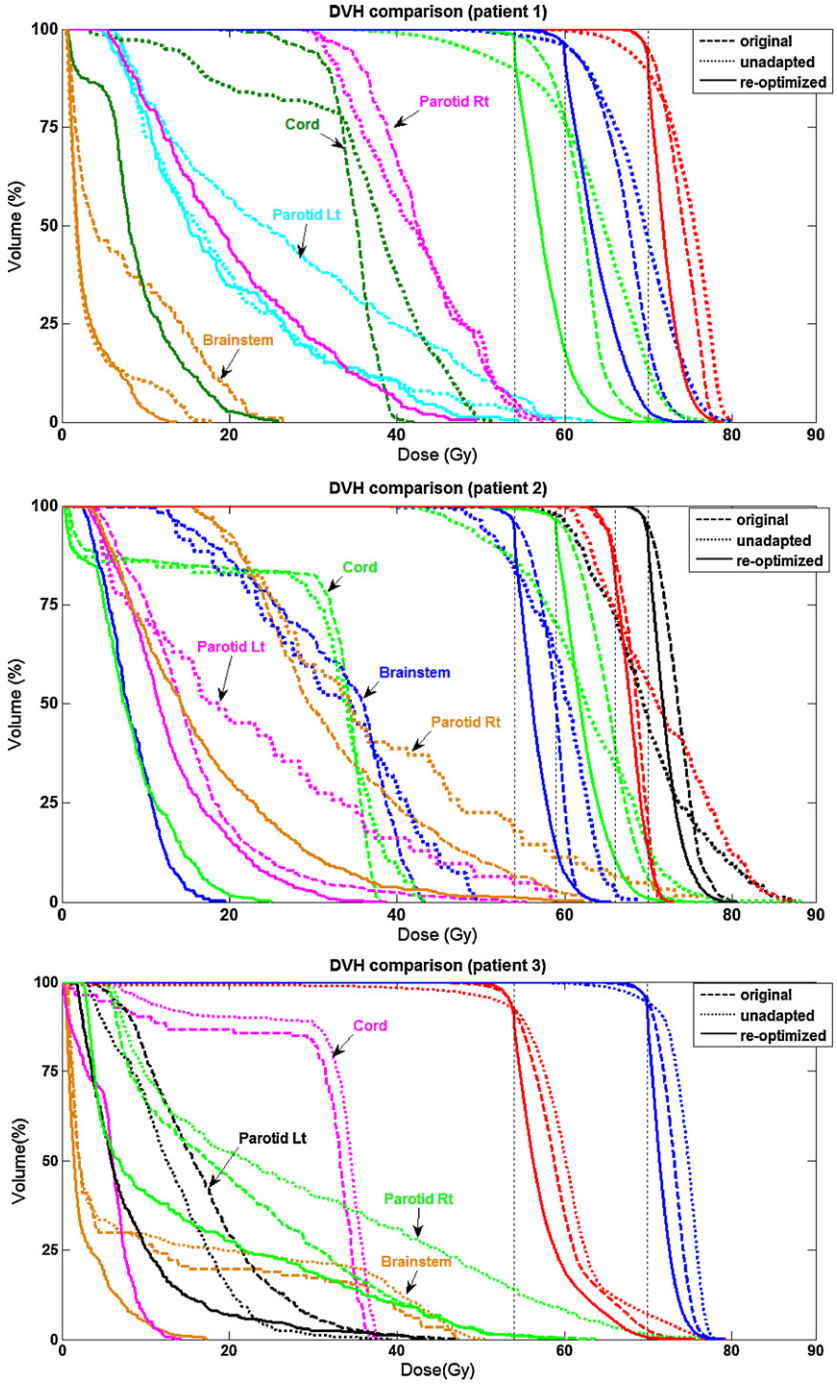

Figure 2. DVH curves comparison. Dashed line: original plan; dotted line: un-adapted plan; Solid line: re-optimized plan.

This strategy keeps the weighting factors within $(0, \sum_{j\in V} w_j^1)$, a range that does not change with iterations. It is worthwhile to mention that the normalization does not affect the optimal solution from the mathematical standpoint.

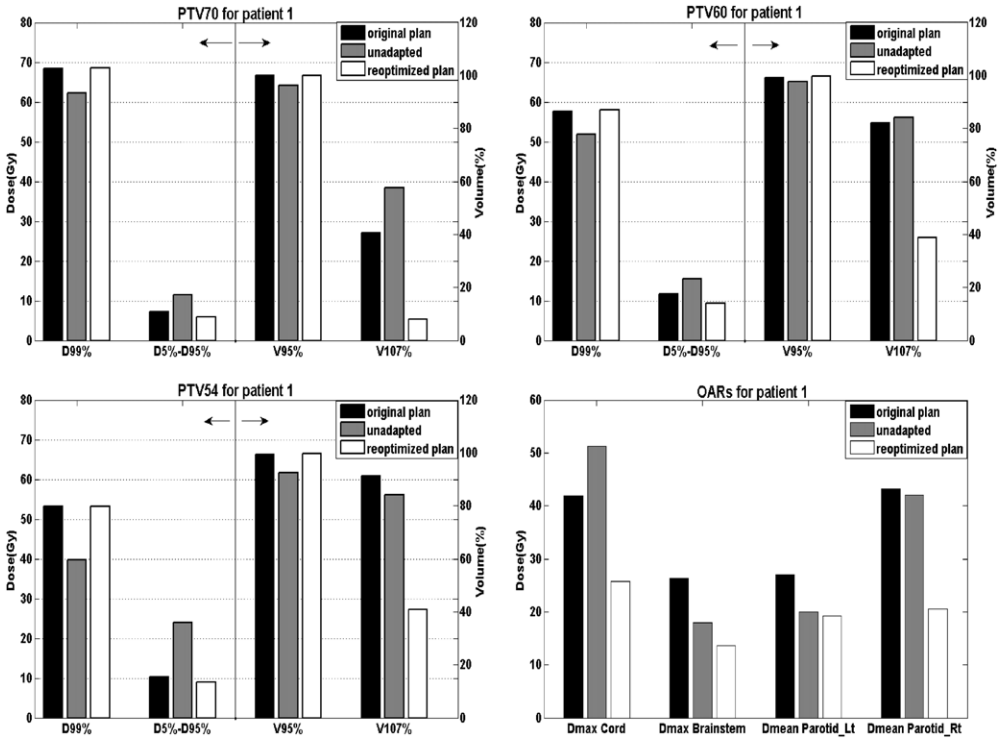

Figure 3. Plan evaluation data for patient 1. Black bar: original plan; gray bar: un-adapted plan; white bar: re-optimized plan.

2.4. Testing cases

We demonstrate the effectiveness of our DVH-guided automatic re-optimization method using three clinical head-and-neck (HN) cancer cases that have received re-simulation and re-planning in the middle of treatment courses. There are two sets of CT images for each patient. The first one is planning CT (pCT) acquired at the initial treatment planning stage, and the second one is called treatment CT (tCT) obtained at the re-planning stage. We refer to the plan corresponding to pCT as the original plan. Contour delineation is always the main time-consuming component for adaptive radiotherapy. Conventionally, deformable image registration methods (Gu *et al* 2010, Zhen *et al* 2012, Gu *et al* 2013) can be used to propagate the contours from pCT to tCT. However, this procedure has not been well established and the new contours on tCT are not completely reliable, requiring a clinician's inspection and often revision. To avoid any uncertainties in the results caused by the inaccurate contours in tCT obtained from a deformable registration algorithm, in this work we use tCT contours manually delineated by clinicians. Detailed information for these three HN cases can be found in table 1, which lists the change of the number of voxels in PTV1, indicating the tumor shrinkage. For all three cases, seven 6 MV IMRT beams were used with beamlet size as 5×5 mm^2 and the voxel size in both pCT and tCT is $2 \times 2 \times 2.5$ mm^3.

To evaluate the results of our method, three different sets of DVHs for each HN case are compared: (1) the original plan, (2) the un-adapted plan (the original plan delivered on tCT), (3) the re-optimized plan using our new algorithm on tCT.

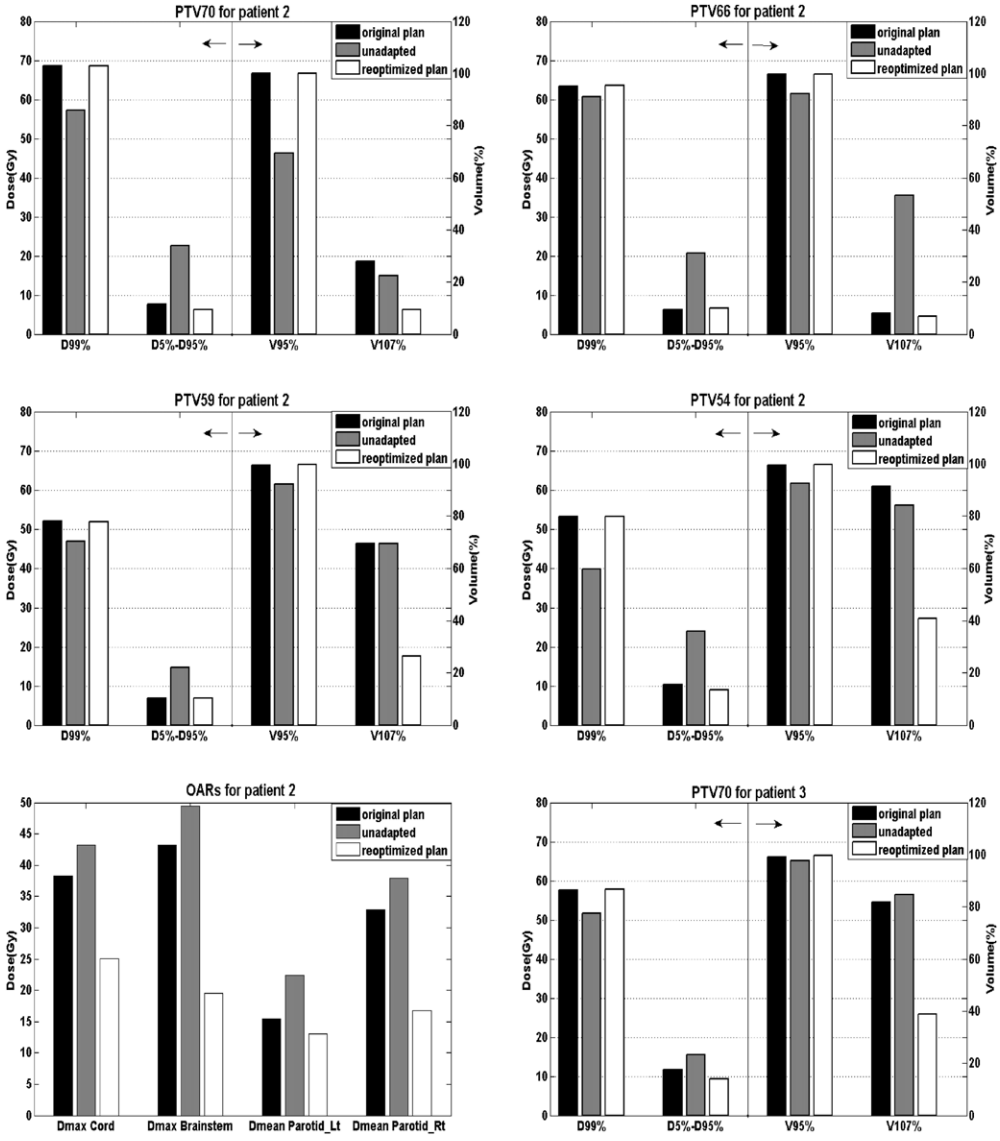

Figure 4. Plan evaluation data for patients 2 and 3. Black bar: original plan; gray bar: un-adapted plan; white bar: re-optimized plan.

3. Results

For these three cases, we adjust the organ weighting factors for the first ten iterations and then adjust the voxel weighting factors for another 20 iterations with parameter μ of 10. The re-optimization process takes about 30 s for 30 iterations using one GPU card for all three cases.

These parameters are empirically chosen through a series of experiments. Firstly, we investigate the impact of iteration numbers for adjusting organ or voxel weights on the convergence of the algorithm. We set the total outer iteration number to be 30, which is always enough to get a good plan based on our experiments. Then by using different combinations

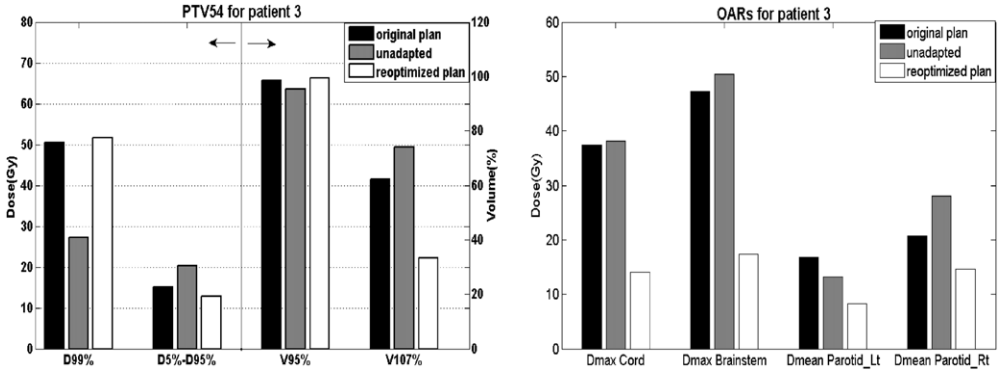

Figure 4. (Continued).

Table 1. Detailed information for three head-and-neck cases.

Case no.	No. of PTVs	Prescribed doses (Gy)	No. of beamlets	No. of voxels in PTV1 (pCT/tCT)
1	3	70, 60, 54	5920	6421/5685
2	4	70, 66, 59, 54	7313	6177/5869
3	2	70, 59	8131	23 172/15 855

of iteration numbers of organ and voxel weight adjusting, we find that by adjusting voxel weights, the algorithm can explore a larger Pareto surface to further improve the plan quality than only adjusting the organ weights, but the convergence speed is much slower. As this test is consistent for different cases, we fix the iteration numbers of the algorithm in our test to adjust the organ weights for the first ten iterations and the voxel weights for the rest 20 iterations, which can make the algorithm to explore a lager Pareto surface while keep a good convergence speed. Then, we tested the convergence performance of the algorithm for different μ values and found that $\mu = 10$ allows the algorithm for a fast convergence performance.

Figure 2 shows the DVHs from the three different treatment plans for each of the three patients. The dashed, dotted and solid curves represent the original, un-adapted and the re-optimized plans respectively. It can be seen that the un-adapted plan is much worse than the original one in terms of the PTV coverage and the delivered dose to cord, indicating that the original plan loses its optimality with the changes in the patient's geometry. After applying our re-optimization technique, the re-optimized plan is even better than the original one in terms of the DVHs. In particular, the PTVs receive more uniform doses and the OARs receive lower doses. In order to make a more clear and detailed comparison, figure 3 shows some plan evaluation data for patient 1. We use D99%, D5%–D95%, V95%, and V107% to evaluate PTV coverage and dose homogeneity. According to these figures, the re-optimized plan has the same D99% and V95% as the original plan, but much lower D5%–D95% and V107%. So our re-optimized plan is the same as the original plan in terms of the PTV coverage, but much better in terms of PTV dose homogeneity. Moreover, the doses are remarkably reduced for organs at risk. The same phenomenon can be observed in the other two patients (see figure 4). These results confirm that our algorithm is able to automatically generate a re-optimized plan that is much better than the un-adaptive one for the patient's new geometry, or even possibly better than the original one.

We also compared the DVHs of the re-optimized plan with the clinically delivered re-plans that generated by dosimetrists based on the treatment CTs, shown as the solid lines and

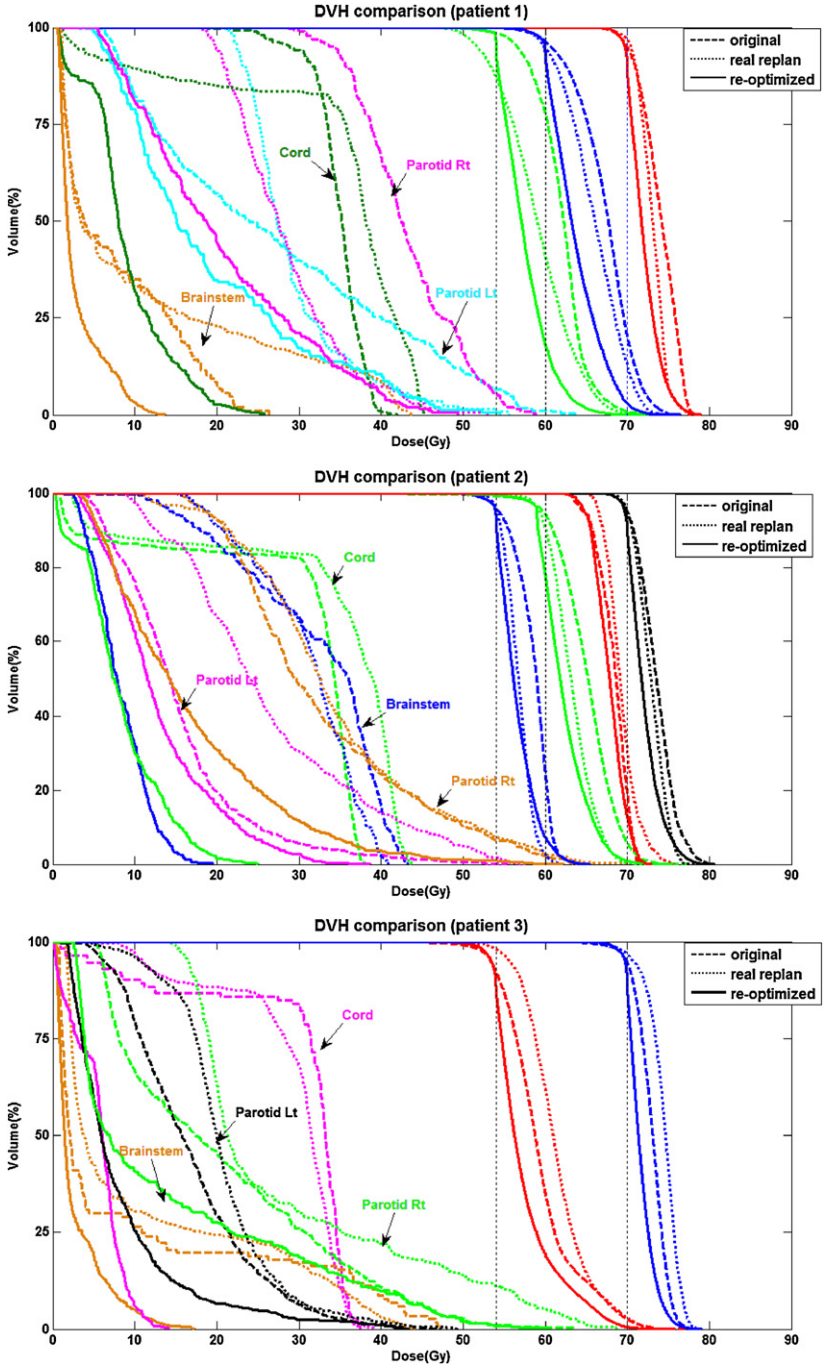

Figure 5. DVH curves comparison. Dashed line: the original plan; dotted line: the clinical delivered re-plan; solid line: re-optimized plan using our new algorithm.

dotted lines in figure 5. We can find that the re-optimized plans using our new algorithm are much better in terms of PTV dose homogeneity and OAR sparing compared with the clinically delivered re-plan while keeping similar PTV coverage. However, there are some hot spots in

our plan for patient 2, which are shown as the tail part of the DVH curves of PTVs. The reason is that the maximum doses in PTV in the original plans, which are used as reference in the proposed method, are higher than that in the clinically delivered re-plans and thus a higher PTV maximum dose is allowed in our re-optimization. In the future work, we will try to modify our algorithm to avoid this kind of problems.

4. Conclusions and discussion

In this paper, we have successfully developed an automatic two-loop algorithm to perform re-optimization of a treatment plan on the patient's new geometry by taking the original DVH into account as guidance. The automated organ and voxel weighting factor adjustments avoid tedious trial-and-error scheme, allowing us to find an acceptable trade-off among different structures for ART re-planning. To verify the effectiveness of our method, we tested it on three HN patients. Promising results have been observed in all three cases tested, such that the re-optimized plans are much better in terms of PTV dose homogeneity and OAR sparing compared with original plans while keeping similar PTV coverage. This algorithm was implemented on GPU so a high computational efficiency has been achieved ($\sim$30 s for a plan re-optimization), making it possible for clinical usage.

This work is very preliminary for using DVH information as the guidance in plan re-optimization. There are still many challenges and a lot of room for improvement. First, the achievability of the original DVHs in the new patient geometry will impact the efficacy of our algorithm. We notice that when the original DVHs are not achievable in the new geometry, the algorithm efficacy will be compromised to a certain extent. Based on our experiments, there are two situations when unachievable DVHs are used as guidance. In one situation, the algorithm will keep increasing the weighting factors for the voxels in the organ with unachievable DVH and sacrificing the DVHs for other structures, and cannot converge to a desired set of DVH curves that are the closest to the original DVHs. However, a more common situation is that the resulting DVHs are still quite reasonable and close to the reference one. So it is still an open question as for how much our algorithm can accommodate unachievable DVHs. A possible reason for this limitation is that there is no stopping strategy in our algorithm to stop increasing the weighting factors when the DVH curve is unachievable and no priorities for different structures in the optimization. So a further study needs to be done to consider the un-achievable DVH curves.

Second, since the relationship between DVH curves and the weighting factors are not clear yet, the way that we adjust the weighting factors is still heuristic and the convergence of the algorithm cannot be guaranteed. More rigorous studies are necessary to discover such a relationship and come up with an appropriate way to adjust the weighting factors. We will explore these directions in our future work.

Another limitation of the proposed method is that the plan quality is only measured by DVHs and totally neglects the spatial dose information. We noticed that some of our good plans in terms of DVH have highest dose in the overlapping part of the PTV and an OAR, which is not desired and may be rejected by physicians when the dose distribution is checked. To solve this kind of problem, spatial dose information should be included in optimization process. We are also working toward this direction and got some promising preliminary results (Uribe-Sanchez *et al* 2012).

When we look at the DVH curves of the re-optimized plan for patient 1, we found an interesting phenomenon, which is that the DVH curves for PTV60 and PTV54 show discontinuities to a certain extent at the prescribed dose value. This means a lot of voxels in these structures receive exactly the prescribed dose value. We found that after 30 iterations,

namely at the end of our algorithm, a lot of voxels have a very high under-dose weighting factors. As a consequence, the dose values for these voxels are pushed to be exactly at the prescribed dose.

We also observed some significant improvements for cord in all the three patients and for the right parotid in patient 1. To better understand this, we did a carefully study using patient 1 as an example. First of all, we compared the contours of the patient on both CT sets. We found that the contours of right parotid delineated by physicians are not perfectly consistent. There are more slices from tCT that contains the right parotid contours, but on each slice it is smaller and has less overlap with PTV than that from pCT. This is one of the reasons for the significant improvement of right parotid, which can also be proved by comparing the original plan with the treated re-plan in figure 5. We also did an experiment to check how optimal the original plan is. We found that there is still some room for improvement, which can be proved by using our method to do re-optimization with the same CT set. Then we imported our re-optimized plan to Eclipse to do dose calculation, which can guarantee a fair comparison when we compare our resulted DVHs with that from the original plan. The results of this experiment proved that the original plan did not push enough on the cord and left a large room for improvement. Another possible reason is that the spatial dose distribution is not used as guidance in our algorithm, making the optimization problem more flexible.

Acknowledgments

This work is supported by the University of California Lab Fees Research Program, a Master Research Agreement from Varian Medical Systems, Inc and the National Natural Science Foundation of China (no. 30970866).

Appendix

Let us consider two dose distributions, namely the current one and the original one, with probability density functions $p_c(d)$ and $p_o(d)$, respectively. According to the definition of a DVH function, the DVHs for these two dose distributions can be written as

$$V_c(d) = \int_d^\infty \mathrm{d}t\, p_c(t),$$
$$V_o(d) = \int_d^\infty \mathrm{d}t\, p_o(t). \tag{A.1}$$

For a given dose level d for the current dose distribution, the mapped dose level d' according to the scheme employed in this paper (see figure 1) satisfies the condition

$$\int_d^\infty \mathrm{d}t\, p_c(t) = \int_{d'}^\infty \mathrm{d}t\, p_o(t). \tag{A.2}$$

We would like to show that after a transformation defined by the above equation, the DVH of the dose distribution of d' is given by V_o.

As such, we first note that if we view equation (A.2) as a definition for an implicit function $d'(d)$, this function is monotonically increasing. This can be easily verified by taking a derivative of equation (A.2) with respect to d, yielding $\frac{\mathrm{d}d'(d)}{\mathrm{d}d} = p_c(d)/p_o(d'(d)) > 0$. Moreover, equation (A.2) can be written as $V_c(d(d')) = V_o(d')$. Now we can compute the DVH function $V(d')$ corresponding to the generated dose distribution d' as

$$V(d') = P(s' > d') = P(s > d(d')) = V_c(d(d')) = V_o(d') \tag{A.3}$$

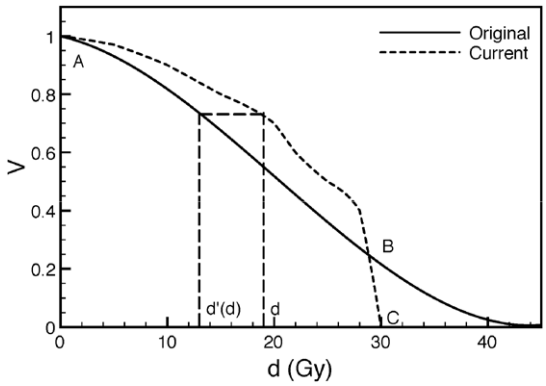

Figure A1. Illustration of mapping the current dose to the original dose based on their DVH curves.

where $P(s' > d')$ denotes the probability that the dose value is greater than d' in the newly generated dose domain and $P(s > d(d'))$ is the probability that the dose value is greater than d in the current dose domain. The second equality follows from the monotonicity of the mapping $d(d')$, while the first and the third one come from DVH definition. Equation (A.3) indicates that after the mapping, the DVH curve for the generated dose distribution is identical to that for the original one.

We finally remark that such a proof is valid wherever the mapping is conducted. For instance, when the current DVH is better than the original DVH, e.g. in the region to the right side of the point B in figure A1, we do not perform the mapping, and hence the DVH in that region is unchanged. Specifically, the generated dose has a DVH curve that follows the solid curve from A to B and then the dashed curve from B to C.

We would like to point out that the proof considers the case of a single organ. If there are multiple organs and they are disjointing of each other, the proof will still be valid. When there are overlaps between the organs, depending on the situation, the proof may not be valid anymore: (1) when the PTV overlaps with an organ, our algorithm gives PTV the highest priority and hence the overlap is not considered in our optimization. Under this circumstance, the proof is still valid. (2) When two organs overlaps, the mapping, as well as the proof do not hold any more, as the mapping for two different organs may conflict with each other at this overlapping area. However, the proof is always valid for the cases we are tested in this paper.

References

Ahunbay E E, Peng C, Chen G P, Narayanan S, Yu C, Lawton C and Li X A 2008 An on-line replanning scheme for interfractional variations *Med. Phys.* **35** 3607

Ahunbay E E, Peng C, Godley A, Schultz C and Li X A 2009 An on-line replanning method for head and neck adaptive radiotherapy *Med. Phys.* **36** 4776

Breedveld S, Storchi P R M, Keijzer M, Heemink A W and Heijmen B J M 2007 A novel approach to multi-criteria inverse planning for IMRT *Phys. Med. Biol.* **52** 6339–53

Cotrutz C and Xing L 2002 Using voxel-dependent importance factors for interactive DVH-based dose optimization *Phys. Med. Biol.* **47** 1659

Cotrutz C and Xing L 2003 IMRT dose shaping with regionally variable penalty scheme *Med. Phys.* **30** 544

Court L E, Dong L, Lee A K, Cheung R, Bonnen M D, O'Daniel J, Wang H, Mohan R and Kuban D 2005 An automatic CT-guided adaptive radiation therapy technique by online modification of multileaf collimator leaf positions for prostate cancer *Int. J. Radiat. Oncol. Biol. Phys.* **62** 154–63

Court L E, Tishler R B, Petit J, Cormack R and Chin L 2006 Automatic online adaptive radiation therapy techniques for targets with significant shape change: a feasibility study *Phys. Med. Biol.* **51** 2493

Feng Y, Castro-Pareja C, Shekhar R and Yu C 2006 Direct aperture deformation: an interfraction image guidance strategy *Med. Phys.* **33** 4490

Fredriksson A 2012 Automated improvement of radiation therapy treatment plans by optimization under reference dose constraints *Phys. Med. Biol.* **57** 7799

Gu X, Choi D, Men C, Pan H, Majumdar A and Jiang S B 2009 GPU-based ultra-fast dose calculation using a finite size pencil beam model *Phys. Med. Biol.* **54** 6287

Gu X, Dong B, Wang J, Yordy J, Mell L, Jia X and Jiang S B 2013 A contour-guided deformable image registration algorithm for adaptive radiotherapy *Phys. Med. Biol.* **58** 1889

Gu X, Jelen U, Li J, Jia X and Jiang S B 2011 A GPU-based finite-size pencil beam algorithm with 3D-density correction for radiotherapy dose calculation *Phys. Med. Biol.* **56** 3337

Gu X, Pan H, Liang Y, Castillo R, Yang D, Choi D, Castillo E, Majumdar A, Guerrero T and Jiang S B 2010 Implementation and evaluation of various demons deformable image registration algorithms on a GPU *Phys. Med. Biol.* **55** 207

Lougovski P, LeNoach J, Ma Y, Zhu L and Xing L 2009 *Adjustable Prescription Dose: A New Strategy to Improve IMRT Treatment Planning* (Berlin: Springer) pp 631–4

Lougovski P, LeNoach J, Zhu L, Ma Y, Censor Y and Xing L 2010 Toward truly optimal IMRT dose distribution: inverse planning with voxel-specific penalty *Technol. Cancer Res. Treat.* **9** 629 PMID: 21070085

Ludlum E, Mu G, Weinberg V, Roach M III, Verhey L J and Xia P 2007 An algorithm for shifting MLC shapes to adjust for daily prostate movement during concurrent treatment with pelvic lymph nodes *Med. Phys.* **34** 4750

Men C, Gu X, Choi D, Majumdar A, Zheng Z, Mueller K and Jiang S B 2009 GPU-based ultrafast IMRT plan optimization *Phys. Med. Biol.* **54** 6565

Mestrovic A, Milette M P, Nichol A, Clark B G and Otto K 2007 Direct aperture optimization for online adaptive radiation therapy *Med. Phys.* **34** 1631

Mohan R, Zhang X, Wang H, Kang Y, Wang X, Liu H, Ang K K, Kuban D and Dong L 2005 Use of deformed intensity distributions for on-line modification of image-guided IMRT to account for interfractional anatomic changes *Int. J. Radiat. Oncol. Biol. Phys.* **61** 1258–66

Schwartz D L 2012 Current progress in adaptive radiation therapy for head and neck cancer *Curr. Oncol. Rep.* **14** 139–47

Shou Z, Yang Y, Cotrutz C, Levy D and Xing L 2005 Quantitation of the *a priori* dosimetric capabilities of spatial points in inverse planning and its significant implication in defining IMRT solution space *Phys. Med. Biol.* **50** 1469–82

Uribe-Sanchez A, Zarepisheh M, Jia X and Jiang S 2012 TU-G-BRB-07: improve PTV dose distribution by using spatial information in IMRT optimization *Med. Phys.* **39** 3920

Wu C, Olivera G H, Jeraj R, Keller H and Mackie T R 2003 Treatment plan modification using voxel-based weighting factors/dose prescription *Phys. Med. Biol.* **48** 2479

Wu Q J, Thongphiew D, Wang Z, Mathayomchan B, Chankong V, Yoo S, Lee W R and Yin F F 2008 On-line re-optimization of prostate IMRT plans for adaptive radiation therapy *Phys. Med. Biol.* **53** 673

Yan D, Vicini F, Wong J and Martinez A 1997 Adaptive radiation therapy *Phys. Med. Biol.* **42** 123

Yang Y and Xing L 2004 Inverse treatment planning with adaptively evolving voxel-dependent penalty scheme *Med. Phys.* **31** 2839

Zarepisheh M, Uribe-Sanchez A F, Li N, Jia X and Jiang S B 2012 A multi-criteria framework with voxel-dependent parameters for radiotherapy treatment plan optimization arXiv:1210.7006

Zhen X, Gu X, Yan H, Zhou L, Jia X and Jiang S B 2012 CT to cone-beam CT deformable registration with simultaneous intensity correction *Phys. Med. Biol.* **57** 6807